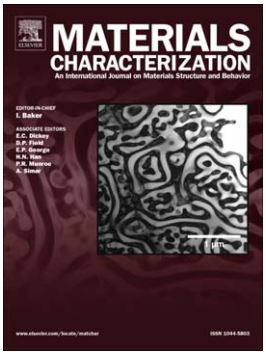

Anisotropy in thermal conductivity of graphite flakes-SiC$_p$/matrix composites: Implications in heat sinking design for thermal management applications

J.M. Molina, E. Louis

PII: S1044-5803(15)00352-6
DOI: doi: 10.1016/j.matchar.2015.09.016
Reference: MTL 8031

To appear in: *Materials Characterization*

Received date: 15 June 2015
Revised date: 21 September 2015
Accepted date: 23 September 2015

Please cite this article as: Molina JM, Louis E, Anisotropy in thermal conductivity of graphite flakes-SiC$_p$/matrix composites: Implications in heat sinking design for thermal management applications, *Materials Characterization* (2015), doi: 10.1016/j.matchar.2015.09.016

Anisotropy in thermal conductivity of graphite flakes-SiC_p/matrix composites: implications in heat sinking design for thermal management applications

J.M. Molina[a,b,c], E. Louis[a,b,d]

[a] *Instituto Universitario de Materiales de Alicante, Universidad de Alicante, Ap. 99, E-03080, Alicante, Spain*

[b] *Departamento de Física Aplicada, Universidad de Alicante, Ap. 99, E-03080 Alicante, Spain*

[c] *Departamento de Química Inorgánica, Universidad de Alicante, Ap. 99, E-03080 Alicante, Spain*

[d] *Unidad Asociada del Consejo Superior de Investigaciones Científicas, Universidad de Alicante, Ap. 99, E-03080 Alicante, Spain*

Abstract

Within the frame of heat dissipation for electronics, a very interesting family of anisotropic composite materials, fabricated by liquid infiltration of a matrix into preforms of oriented graphite flakes and SiC particles, has been recently proposed. Aiming to investigate the implications of the inherent anisotropy of these composites on their thermal conductivity, and hence on their potential applications, materials with matrices of Al-12wt.%Si alloy and epoxy polymer have been fabricated. Samples have been cut at a variable angle with respect to the flakes plane and thermal conductivity has been measured by means of two standard techniques, namely, steady state technique and laser flash method. Experimental results are presented and discussed in terms of current models, from which important technological implications for heat sinking design can be derived.

Keywords: A. Metal-matrix composites (MMCs); A. Polymer-matrix composites (PMCs); B. Anisotropy; B. Thermal properties

---

Corresponding author: J.M. Molina (jmmj@ua.es)

1. Introduction

Graphite-based composites constitute nowadays an important family of materials with a great range of applications [1-5]. In these materials, graphite is present as second phase in different shapes: particles, short fibres, foams, flakes, nanotubes, etc. With the exception of those particles formed either by isostatically pressing smaller particles or either by folding up graphite flakes, the rest are intrinsically anisotropic. This anisotropy is normally transferred to the macroscopic properties of these materials. However, many graphite-based composites, especially those fabricated with reinforcements of short dimensions, are typically isotropic due to the fact that there is no massive orientation of their graphitic second phases. These materials, owing to the randomization of the anisotropic properties of their second phases, have relatively poor properties. In fact, the main problem posed by the various carbon reinforcements evaluated in the last twenty years (graphite particles, short carbon fibres or carbon nanotubes) seems to be the difficulty in getting massive orientation to take benefit of the exceptional planar (two-dimensional) properties of graphite [6-9].

One of the applications for which graphite-based composites have been mostly evaluated concerns their use as heat sinks for thermal management in electronics. Compared to their direct candidate competitors (copper matrix composites and Al/SiC), several are the advantages that these materials offer: low price, low weight and ease of machinability. Nevertheless, until recently, these materials were mainly limited by their low values of thermal conductivity (TC). The use of graphite as a key component of materials for thermal management has been recently triggered by a novel proposal, in which metal matrix graphite flakes-based composites have been fabricated by pressure-assisted infiltration [4,5,10,11]. Packaging and infiltration of graphite flakes is a delicate process due to intrinsic problems related to the flakes morphology. Packing of the flakes by a common uniaxial pressing procedure tend to orient them in such a way that they lie on top of each other, conforming a relatively dense preform with no open channels to allow infiltration of the liquid metal, necessary to consolidate the material. This difficulty has been solved by a new method developed by the authors [12-17] that consists of preparing and packing powder mixtures conformed by a combination of graphite flakes and another finely divided material with a largely different morphology (i.e. SiC particles or carbon fibers). When packed, these mixtures tend to naturally adopt a microstructure in which graphite flakes get oriented in planes and in between the planes the material with different morphology is confined, acting as a separator. The material can be described as

a three-phase composite that, based on its properties, is clearly anisotropic given the intrinsic properties of the graphite flakes and their orientation in the preform. Within such a microstructure, the thermal conductivity is highest along the two directions parallel to the oriented flakes plane. For this plane, the coefficient of thermal conductivity exhibits its lowest value. The parameters affecting the overall thermal conductivity of these materials are many and, hence, have to be conveniently controlled: purity of metal and reinforcement phases, reactivity between matrix and reinforcement, dimensions and aspect ratio of graphite flakes, orientation and degree of alignment of graphite flakes, etc.

Oriented graphite-flakes heat spreaders can take advantage of the anisotropic thermal properties of natural graphite and, adequately implemented in electronic packaging, can act as both, heat spreaders or thermal insulators, to eliminate localized hot spots in electronic components. Both experimental techniques and numerical models have been used to examine performance of anisotropic heat spreaders for these applications. In a simplified model, Tzeng [18] showed that an anisotropic heat spreader, with properties similar to those of natural graphite, could lower the maximum temperature of a localized heat source by proper transfer of heat from an electronics enclosure to an external mounting rack. Design of proper placement and orientation of anisotropic heat sinks is mandatory in order to create an adequate heat extraction, since there is the risk that the case temperature immediately below the heat source can be high. One of the most recent examples of use of an anisotropic graphite-based heat spreader is that described by Norley in [19], which consists of chemically bonded expanded natural graphite with an in-plane TC up to 230 W/mK and a perpendicular TC of 4.5 W/mK. The use of resin to fill in the porosity leads to an increase of the perpendicular TC up to 70 W/mK. Due to the low TC of non-metallic matrices, metals are preferred as matrix materials to build up composites with high TC.

The present contribution is addressed to evaluate the implications of the inherent anisotropy of the recently developed G_f-SiC_p/matrix composites [12-17] by considering two largely different thermally conductive matrices: Al-12wt.%Si alloy and epoxy resin. The evaluation of the anisotropy of the composite was carried out by cutting samples out from primigenial pieces (one for each matrix type) at a variable angle θ with respect to the flakes plane, and measuring their thermal conductivity. The fact that all samples with same matrix come from a single piece of material serves to insure that the only differentiating feature among them is the orientation of graphite fakes along the measurement axis. The results here presented have aspects of technological relevance. Specifically, while for angles 0º and 90º (perpendicular and parallel to the graphite flakes, respectively) the thermal conductivity does not depend

on the shape of the sample; a significant dependence is found for intermediate angles. In addition, it is shown that samples are microstructurally inhomogeneous for length scales shorter than 600 μm. The results provide useful information on how an error when orienting the samples for final cutting may affect final properties. These features suggest that, although *in situ* evaluation seems somehow necessary, lab testing may give a precise indication of what the material properties are and how to implement these materials as heat sinks in electronics.

2. Experimental Procedures

2.1 Materials

Composites were prepared by infiltrating a liquid matrix into preforms of graphite flakes (G_f) and silicon carbide (SiC_p) particles mixtures. Graphite flakes were purchased from Graphitwerk Kropfmühl AG (Hauzenberg, Germany). They have platelet morphology with the following dimensions: 400 μm of average diameter and 50 μm of average thickness. Silicon carbide particles, of green quality (>99%), were kindly donated by the Spanish company Navarro SiC S.A. (Cuenca, Spain). Particles with average diameters over the range 12.7-167 μm were used. The respective morphologies of graphite flakes and SiC particles are illustrated by the micrographs of Figures 1a and 1b. From Figure 1a it becomes evident the clear platelet morphology of the graphite flakes, which exhibit clean flat base surfaces. SiC particles are irregular but clearly more rounded (image analysis gives aspect ratios of 12 and 1.6 for flakes and particles, respectively). Preforms were infiltrated either with the eutectic alloy Al-12wt%Si (hereafter referred to as Al-12Si), supplied by LKR Leichtmetallkompetenzzentrum Ranshofen GmbH (Ranshofen, Austria), for which chemical analysis revealed 0.1% Fe as major impurity, or with WWA epoxy resin (with WWB4 hardener), supplied by Resoltech SAS (Eguilles, France).

2.2 Composites Fabrication

The fabrication procedure selected for composite fabrication was liquid metal infiltration assisted by gas pressure. Prior to infiltration, preparation and packing of the particle mixtures turns to be a delicate and tricky process that requires personnel with the necessary experience. Preparation of the mixtures was

carried out by mixing the proper amounts of graphite flakes and SiC particles in a container with cyclohexane. The suspension was magnetically stirred for at least 30 minutes, after which the samples were dried in a conventional oven at 70ºC. Once dried, the mixtures were packed by pouring them into steel moulds of dimensions 60x60x30 mm and by applying a uniaxial pressure of 40 bars with the help of a hand-pressing machine.

Pressing direction was *y* while the *xz* was the flakes plane (Fig.2). This method facilitates two essential requisites of the mixture preforms, namely, orientation of graphite flakes and alternation of SiC particles and oriented flakes. As already explained, packing of flakes and SiC particles into the moulds turns out to be the most demanding step of the composite fabrication. Measuring the weight and the exact dimensions of the packed preforms allowed obtaining the volume fraction of each component.

The packed preforms were subsequently placed in cylindrical crucibles made out of stainless steel, whose internal surface was covered with a thin layer of a boron nitride-based painting that is delivered as aerosol paint (ZYP Coatings Inc,, Oak Ridge, EEUU). In order to fill the space in between preform and crucible, a fine graphite powder was poured and packed with the help of a small piston used as hammering tool.

Different procedures were followed for metal and polymer infiltrations. For infiltration with Al-12Si alloy, a solid piece of the metallic alloy was placed on top of the packed preform and, prior to melting, the sample was transferred into a cold-wall heating chamber where primary vacuum was applied in order to facilitate infiltration and reduce porosity (see [20,21] for equipment details; see [10,17,21,22] for details on infiltration process). Then, the temperature was raised up to 700ºC (Al-12Si alloy) and nitrogen was introduced into the pressure chamber until a pressure of 25 bars was reached. After two minutes of infiltration, the heating was stopped and the sample was let for slow solidification. For infiltration with epoxy resin, the G_f-SiC_p packed preform was placed in a small desiccant container properly adapted for resin moulding. Primary vacuum was applied and afterwards the liquid epoxy resin was poured on top of the packed preform. The chamber was open and the sample was transferred into the cold-wall heating chamber (the one used, as described above, for metal infiltrations). A pressure of 25 bars (at a temperature of 25ºC, this is, with no extra heating) was applied for two days, in order to achieve infiltration and curing of the resin. After infiltration, samples were cut out from the infiltrated pieces along a direction forming an angle θ with the flakes plane (plane xz). Figure 2 illustrates the cutting process.

2.3 Materials characterization

2.3.1. Microstructure - Image analysis characterization

Representative samples were sectioned and mounted in thermosetting resin (Buehler Diallyl Phthalate resin, from Buehler, Illinois, USA). Standard metallographic techniques for optical microscopy were followed. Grinding was done with the help of a water-lubricated rotating disk covered with silicon carbide papers of subsequent decreasing granularity (P120-P240-P400-P800-P1200 and P2500, each stage lasting for approximately 10 min). Polishing was achieved by using a silk cloth and diamond paste as abrasive (from Buehler, Illinois, USA). Three different abrasive diamond pastes of 15, 6 and 1 μm were used in consecutive steps that lasted 30 min each.

In these materials it is very interesting to study not only the anisotropy but also the inhomogeneity in their microstructure. Both characteristics are especially important in heat sinking design for applications in electronics. Anisotropy is important for the heat sink assembly and hence knowledge of proper graphite flakes angle with respect to sample geometry is also important. Inhomogeneity, which may be determinant to know the limitations of a material to be used for heat extraction, can be measured by the degree of misalignment of the flakes and the minimum size of a specimen for which the measurement of volume fraction of the different phases is constant. These measurements were carried out with image analysis software, from Buehler-Omnimet Enterprise (Illinois, USA), coupled to an Olympus PME-3 optical microscope. For doing so, it was necessary to work with image fields that covered representative areas of the samples. Given that the lowest magnification of the optical microscope was high for this purpose (50x), sets of several images at 50x were taken and then joined with the software of the Image Analysis in order to have image fields of 1200 μm x 1600 μm. The different constituent phases were differentiated by thresholding the images based on a grey-scale criterion. The measurements were carried out in at least ten groups of composed picture sets in order to access to statistics on the material.

2.3.2. Thermal conductivity

The thermal conductivity was measured by means of two techniques, namely, the relative steady-state technique (RSST), and the laser flash test (LFT). RSST measurements were carried out on paralellepipedic samples of 25 mm height and a square section of side 10 mm, in a non-commercial

equipment assembled at the laboratories of the University of Alicante by following the ASTM E1225-04 International Standard [21]. The equipment basically consists of a clamping system able to establish a thermal gradient over a sample and a reference that are in contact across their cross sections. The reference material is in contact with a copper block that in its turn is connected to a thermally stabilized hot water bath at 70ºC. The sample is connected to a water-cooled copper block at 20ºC. Reference and sample are protected with thermal insulating materials in order to insure that heat losses through radiation and/or convection are minimized. For those samples having Al-12Si as matrix, a reference of oxygen-free high purity copper (99.999%), with a nominal thermal conductivity of 398 W/mK at 40ºC, was used. Alternatively, brass alloy, with a thermal conductivity at 40ºC of 120 W/mK, was used as reference when dealing with samples containing epoxy resin as matrix.

Both references were of cylindrical shape, with a diameter of around 16 mm and length of 40 mm. The overall error associated with these measurements was estimated to be less than 5%.

LFT measurements in turn were carried out in a Netzsch LFA 457 apparatus (located at the laboratories of CEIT, San Sebastián, Spain) on samples of 2 mm thick and a circular section of diameter 10 mm. The measurement basically consists of irradiating one face of the sample by a short laser pulse ($\leq$ 1 ms) and measuring the temperature rise on the opposite face of the sample. Standard algorithms were used in order to correct heat losses through radiation during the measurement [23]. The thermal diffusivity of the sample could be derived from the profile of a temperature vs time graph. By using the equation $K = \alpha C_p \rho$, with α being the thermal diffusivity and C_p and ρ being the specific heat at constant pressure and density, respectively, the thermal conductivity K of the sample was easily calculated. When C_p is unknown, as it is the case in the present study for the different materials fabricated, the linear rule of mixtures can offer a good approximation (see [13] for details).

3. Modelling

The experimental results were interpreted with the aid of current approaches to describe the angular dependence of the thermal conductivity of anisotropic solids [24-26]. For that sake, let us assume that a thermal gradient is applied along the z-direction in the x-z plane (note that in oriented structures like the one of the material herewith discussed, the x and y directions are equivalent). Being the direction cosines of the z-axis relative to the principal axes of conductivity (in this case the axes parallel and perpendicular

to the graphite planes), $\cos\theta$ and $\sin\theta$, the relevant components of the second rank conductivity tensor, are [25]:

$$K_{zz}(\theta) = K^L cos^2(\theta) + K^T sin^2(\theta) \quad (1a)$$

$$K_{xz}(\theta) = K_{zx}(\theta) = (K^L - K^T) sin\theta cos\theta \quad (1b)$$

$$K_{xx}(\theta) = K^L sin^2\theta + K^T cos^2\theta \quad (1c)$$

where K^L and K^T are the thermal conductivities of the composite in the directions parallel and transversal to the flakes plane. In the case of an infinite thin plate with the thermal gradient perpendicular to it, the thermal conductivity of the composite can be closely approximated by $K_{zz}(\theta)$ [25]:

$$K_c(\theta) \approx K_{zz}(\theta) \quad (2)$$

If, instead, the sample is infinitely long along the heat gradient direction z, being insulated along its length, heat will be forced to flow solely in the z-direction and the conductivity of the composite will be given by [24,26]:

$$K_c(\theta) = K_{zz}(\theta) - \frac{K_{xz}^2(\theta)}{K_{xx}(\theta)} \quad (3)$$

On the other hand, the direction of heat flow (note that in anisotropic materials the heat flow direction may not coincide with the direction of the temperature gradient, see [24]) forms an angle ϕ with the flakes plane, given by:

$$tan\varphi = \frac{K^T}{K^L} tan\theta \quad (4)$$

Two limiting cases of interest are: a) $K^T = K^L$, then $\phi = \theta$, and b) $K^L >> K^T$, then $\phi=0$.

It should be noted that while the TC was calculated by means of both Equations (2) and (3), K_T and K_L in Equations (1-4) can be calculated by means of a model that considers oriented graphite flakes, shaped as disks, in a pseudo-matrix consisting of a binary composite of SiC particles and Al-Si alloy or epoxy resin. This model of oriented disks was first proposed by Hatta and Taya and takes the following form:

$$K^i = K_{mp} + K_{mp} \frac{V_f}{S^i(1 - V_f) + \frac{K_{mp}}{K_f^i - K_{mp}}} \quad (5)$$

where the superscript i= L,T refers to longitudinal and transversal directions (related to the flakes plane) and S^i is a geometrical factor whose value depends on both the morphology and orientation of the reinforcement. K_{mp} is the thermal conductivity of the pseudo-matrix, which can be calculated with the mean field approach (DEM model) as follows:

$$(1 - V_p) = \frac{(K_p^{eff}/K_m) - (K_{mp}/K_m)}{(K_p^{eff}/K_m) - 1} \left(\frac{K_{mp}}{K_m}\right)^{-\frac{1}{3}} \quad (6)$$

K_p^{eff} is defined in turn as

$$K_p^{eff} = \frac{K_p}{1 + \frac{K_p}{rh}} \quad (7)$$

where K_p and r refer to the intrinsic thermal conductivity and the average radius of the SiC particles, considered as spheres, respectively; *h* is the thermal conductance of the Al-Si/SiC_p interface.

The expressions for calculating S^i for the present case where flakes builds up a network of oriented thin disks distributed in the matrix-SiC_p composite, are the following:

$$S^L = \frac{\pi t}{4D} \quad (8)$$

$$S^T = 1 - \frac{\pi t}{2D} \quad (9)$$

where t is the thickness of the graphite flakes and D their average diameter.

In calculating K^T, the thermal conductivity of the graphite flakes must be replaced by an effective value which is calculated by an expression equivalent to (7):

$$K_f^{T,eff} = \frac{K_f^T}{1 + \frac{K_f^T}{th_{fmp}}} \quad (10)$$

4. Results and discussion

4.1. Microstructure and Image analysis characterization

A representative optical micrograph of the composites obtained at the lowest possible magnification of 50x is shown in Figure 3a. Figure 3b shows an image of the microstructure of the material that covers a total area of 1200 μm x 1600 μm, which has been obtained by joining with the Image Analysis software nine consecutive images of low magnification (50x) as the one in Fig 3a. The microstructures shown in Figure 3 reveal the morphologies and spatial distribution of graphite flakes and SiC particles in the matrix of Al-12Si alloy. The graphite flakes conform a quasi-continuous structure of randomly distributed oriented disks while the SiC particles appear with no special orientation together with the metallic matrix in the space in between the flakes. Particles appear homogeneously distributed in the matrix with no

evidence of particle breaking. No evidences of porosity presence are detected, probably due to the vacuum applied to the preform before infiltration, and to the high pressures used for infiltration (25 bars). To evaluate size scale beyond which the composite can be considered homogeneous, the volume fraction of flakes was determined by means of Image Analysis within squared screening windows of increasing size (starting from 50×50 μm) (Fig. 4a). Misalignment of flakes in the microstructure can be determined by the measurement, with the help of Image Analysis, of the orientation of many particular flakes in respect to virtual lines drawn parallel to the cutting plane of the sample (Fig. 4b).

Figures 5 and 6 collect results concerning homogeneity in the volume fraction of the present phases and misalignment of the graphite flakes, respectively, in a sample fabricated by infiltration of Al-12Si into preforms containing 54% of graphite flakes and 29% of SiC particles of an average diameter of 22.5 μm (here below referred as D7 – see Table 1). Results shown in Figure 5a clearly indicate that beyond 400-600 μm of screening window side, the system can be considered homogeneous. This is more clearly seen if the standard deviation of these results is plotted (Figure 5b). It is seen that, albeit the standard deviation should vanish as the size of the square field tends to infinity, beyond 400-600 μm it becomes already very small (smaller than 0.05). This somehow supports the use of samples 2 mm thick in the evaluation of the thermal conductivity by means of the laser flash test (see below).

Figure 6 shows the compilation of such measurements in terms of the probabilistic frequency for a graphite flake to be at a certain angle in respect to the characteristic cutting angle. The figure contains the fittings of experimental data with curves that obey the mathematical expressions for Gaussian functions. From the expressions of the derived fittings the standard deviation of the graphite flakes angle alignment in respect to the cutting angle can be obtained. These values are of 12º for the two curves shown in Figure 6. Measurements carried out in other samples for different cutting reference angles show that the values of standard deviation are always below 15º. The material can be considered as composed of relatively well-oriented graphite flakes and seems adequate for confrontation with predictive models.

4.2 Thermal conductivity – experiments and modelling

Using Equations (1-6) for the modelling of anisotropy in the present composite materials requires an appropriate knowledge of the graphite flakes conductivities, both in the parallel and the perpendicular directions to the basal plane. Given that the direct measurement of these magnitudes is extremely difficult

and cannot be conceive it here, their values may be derived with indirect calculations based on the thermal characterization of these composites in the parallel and the perpendicular directions of flakes orientation. Experimental results for the thermal conductivity of several composites, which differ in their matrix nature and size and content of the SiC particles, as measured by means of the RSST technique are reported in Table 1. K_f^L and K_f^T (thermal conductivities in the parallel and transversal direction of the graphite basal planes of the flakes, respectively) can be derived by linear fittings from plots of the calculated thermal conductivities (with Equations 5-10) versus the experimental thermal conductivities gathered in Table 1. For the calculations, the parameters collected in Table 2 have been used. While V_{SiC} in Table 1 refers to the total volume fraction of SiC particles in the composite, it is interesting to note that the local volume fraction of the SiC particles (V'_{SiC}) in the pseudo-matrix of SiC_p/Al-Si or SiC_p/epoxy, calculated as $V'_{SiC}=V_{SiC}/(1-V_f)$, is in the range 0.52-0.58 (these are two limiting values of the particle volume fraction in the binary composite; for simplicity reasons, an average value of 0.55 can be taken). Figure 7 shows these plots in which it becomes evident that the thermal conductivities of the G_f-SiC_p/epoxy composites are much lower than those corresponding to the G_f-SiC_p/Al-12Si composites. K_f^L is calculated to be 523 W/mK while K_f^T is around 28 W/mK, both values characterizing the anisotropy of the graphite flakes used in the present work. These values are in line with those obtained in ref [9] for composites G_f-SiC_p/Al-12Si. The fact that a unique value of the intrinsic thermal conductivity for the graphite flakes can be derived from composites with matrices of so different nature (metallic alloy and epoxy polymer) denotes that the postulation of considering the flakes as disk-like shaped second phases and the application of the corresponding model to these composites are reasonable approximations.

Table 3 and Figure 8 collect the experimental data of thermal conductivity for the G_f-SiC_p/Al-12Si and G_f-SiC_p/epoxy composites for samples corresponding to preform code D7, obtained by cutting the infiltrated pieces along a direction forming an angle θ with the flakes plane (plane xz), as shown in Figure 2. Anisotropy has been evaluated by the evolution of the thermal conductivity with the flakes orientation. In order to consider the effect of the geometry of the samples, measurements were taken with the two techniques of RSST and LFT, which require largely different sample dimensions.

The measured values for the dependence of the thermal conductivity on flakes orientation for the two series of specimens (G_f-SiC_p/Al-12Si and G_f-SiC_p/epoxy) follow a tendency that is similar to that obtained for uniaxial carbon fiber-reinforced glass matrix composites [24]. In all cases the TC decreases steadily with the angle θ. As it is obvious, the thermal conductivities of both G_f-SiC_p/epoxy and G_f-

SiC_p/Al-12Si composites in the direction parallel to the flakes orientation are well above those obtained for the perpendicular direction, existing a soft transition between these two values with the cutting angles. It is worth commenting that the difference between the two extreme values for parallel and perpendicular directions is about 300 W/mK and about 90 W/mK for G_f-SiC_p/Al-12Si and G_f-SiC_p/epoxy composites, respectively. This difference, that intrinsically characterizes the anisotropy of the material, would have been expected to be much larger if the orientation of the flakes would have been greater.

Furthermore, the above results indicate that the dependence of thermal conductivity on graphite flakes orientation is a function of specimen geometry; i.e. the ratio of its dimension in the direction of heat flow and its width. These results are in perfect agreement with previous studies carried out on composites with continuous fibre reinforcements [24]. For "thin" samples like those required in the LFT measurements, the width of the specimens is much larger than their thickness in the direction of temperature gradient. The conduction of heat flow is unaffected by the edges of the sample and the thermal conductivity behaves as that for a composite sample with infinite dimensions. In consequence, thermal conductivity can be closely approximated with Equation 2. Instead, for samples having a width of the order of its length, or much shorter, like those used in the RSST characterization, heat conduction is affected by the specimen sides, which are thermally isolated from the surrounding medium and constitute heat flow barriers. For these reasons, Equation 3, which is valid for strip-isolated samples, can closely approximate the thermal conductivity. This is to be expected, since the heat is preferentially conducted by the graphite flakes, which are much better thermal conductors than the matrix, being this either Al-12Si or epoxy, and a fraction of the flakes will orient the heat towards the isolated sides of the sample, rather than towards the opposite face of the specimen.

4.3 Heat sinking design considerations

The experimental results above presented have intrinsic relevant interest for the materials development community, as well as they bring technological implications for heat sinking design. Heat sinking design has become a topic of great interest for the control of heat flow in thermo-electronics, the development of thermal circuits for electro-mechanical systems and thermal energy harvesting.

The graphite flakes-based composite materials here presented are clearly anisotropic and their values of thermal conductivity strongly depend on the angle of the oriented flakes in respect to the thermal

gradient. For extreme angles of 0º and 90º there is no extra dependence on specimens shape. However, for intermediate angles, the thermal conductivity is dependent on the geometry of the specimen. While "thin" samples behave as infinite solids, "thick" samples are strongly affected by their surrounding environment and have a sharper decrease of thermal conductivity with the orientation of graphite flakes for intermediate angles, being especially lower for angles close to 45º. This sample-shape dependence should be taken into account when designing a particular heat sink. In general for anisotropic solids, it is preferred the use of "thin" specimens when the design for heat sinking implies the orientation of the graphite flakes at a certain angle, especially for angles close to 45º. In particular for the graphite flakes-based material at hand, there is a limitation in using "thin" specimens as heat sinks: by considering phase constituents homogeneity criterion, the thickness must always be greater than 600 μm. Another implication that is derived from the experimental data herewith presented is that when design criteria impose the use of "thick" specimens, it is preferable that the specimens are embedded in a thermal conductive case in order not to constrict the heat flow through the composite material only in the direction parallel to the thermal gradient, since this would greatly decrease the effective thermal conductivity of the heat sink in this direction.

5. Conclusions

The anisotropy of the recently developed graphite-based three-component composite materials has been evaluated through measurements of the thermal conductivity on samples cut in a direction forming a variable angle with the oriented flakes plane. The results have been discussed in terms of current theoretical approaches. Some issues of technological relevance derived from the present investigation have been identified. Specifically, while for angles 0º and 90º (perpendicular and parallel to the graphite flakes, respectively) the thermal conductivity does not depend on the shape of the sample, a significant dependence has been measured for intermediate angles. In addition, it is shown that samples are inhomogeneous for length scales shorter than 600 μm, being this value a limiting factor when designing "thin" specimens for heat sinking applications. When dealing with "thick" samples of this material for heat dissipation, other considerations must be taken into account, like the possible benefits of encapsulating the material in order to enhance the thermal transport, which otherwise can be poor, specially for intermediate angles. These features indicate that although lab testing may give a precise

indication of what the material properties are, it seems advisable to carry out *in situ* evaluation of its performance.

Acknowledgements

The authors acknowledge partial financial support from "*Ministerio de Ciencia e Innovación" (grant MAT2011-25029), "Universidad de Alicante" and "Generalitat Valenciana"*. J.M. Molina also acknowledges "*Ministerio de Ciencia e Innovación"* for a *Ramón y Cajal* contract.

References

[1] Oku T, Kurumada A, Sogabe T, Hirahako T, Kuroda K. Effects of titanium impregnation on the thermal conductivity of carbon/copper composite materials. J Nucl Mater 1998;257:59-66.

[2] DeVincent SM, Michal GM. Improvement of thermal and mechanical properties of graphite/copper composites through interfacial modification. J Mater Eng Perform 1993;2:323-331.

[3] McCoy JW, Vrable DL. Metal-matrix composites from graphitic foams and copper. SAMPE J 2004;40:7-19.

[4] Rodríguez-Guerrero A, Sanchez S A, Narciso J, Louis E, Rodriguez-Reinoso F. Pressure infiltration of Al–12 wt.% Si–X (X = Cu, Ti, Mg) alloys into graphite particle preforms. Acta Mater 2006;54:1821-1831.

[5] Molina JM, Rodríguez-Guerrero A, Bahraini M, Weber L, Narciso J, Rodríguez-Reinoso F, Louis E, Mortensen A. Infiltration of graphite preforms with Al–Si eutectic alloy and mercury. Scripta Mater 2007;56:991-994.

[6] Agari Y, Ueda a., Nagai S. Thermal conductivity of a polyethylene filled with disoriented short-cut carbon fibers. J Appl Polym Sci 1991;43:1117–24.

[7] Fu SY, Mai YW. Thermal conductivity of misaligned short-fiber-reinforced polymer composites. J Appl Polym Sci 2003;88:1497–505.

[8] Huang H, Liu C, Wu Y, Fan S. Aligned carbon nanotube composite films for thermal management. Adv Mater 2005;17:1652–6.

[9] Wang M, He J, Yu J, Pan N. Lattice Boltzmann modeling of the effective thermal conductivity for fibrous materials. Int J Therm Sci 2007;46:848–55.

[10] García-Cordovilla C, Louis E, Narciso J. Pressure infiltration of packed ceramic particulates by liquid metals. Acta Mater 1999;47:4461-4479.

[11] Molina JM, Prieto R, Duarte M, Narciso J, Louis E. On the estimation of threshold pressures in infiltration of liquid metals into particle preforms. Scripta Mater 2008;42:243-246.

[12] Prieto R, Molina JM, Narciso J, Louis E. Fabrication and properties of graphite flakes/metal composites for thermal management applications. Scripta Mater 2008;59;11-14.

[13] Prieto R, Molina JM, Narciso J, Louis E. Thermal conductivity of graphite flakes–SiC particles/metal composites. Compos A: Appl Sci Manuf 2011;42:1970-1977.

[14] Narciso J, Prieto R, Molina JM, Louis E. Producción de materiales compuestos con alta conductividad térmica. Patent. Ofician Española de Patentes y Marcas. Patent number: ES2304314 (2007).

[15] Narciso J, Prieto R, Molina JM, Louis E. Three phase composite material with high thermal conductivity and its production, European Patent, Patent number: EP2130932-B1 (2007).

[16] Narciso J, Prieto R, Molina JM, Louis E. Production of composite materials with high thermal conductivity, PCT Patent, Application number: WO2008116947-A1 (2008).

[17] Molina JM. SiC as base of composite materials for thermal management. In: Mukherjee M, editor. Silicon carbide-materials, processing and applications in Electronic Devices. ISBN: 978-953-307-968-4, InTech, DOI: 10.5772/20543, 2011. p. 115-140.

[18] Tzeng JW, Getz G, Fedor BS, Krassowski DW. Anisotropic Graphite Heat Spreader for Electronics Thermal Management. In: Proceedings of PCIM Conference. Nuremberg, June, 2000. p.183-188.

[19] Norley J, Tzeng JW, Getz G, Klug J, Fedor B. The development of a natural graphite heat-spreader. In: Proceedings of the Seventeenth IEEE SEMI-THERM Symposium. San José, March, 2001. p.107-110.

[20] Molina JM, Saravanan RA, Arpon R, García-Cordovilla C, Louis E, Narciso J. Pressure infiltration of liquid aluminium into packed SiC particulate with a bimodal size distribution. Acta Mater 2002;50:247-257.

[21] Molina JM, Piñero E, Narciso J, García-Cordovilla C, Louis E. Liquid metal infiltration into ceramic particle compacts chemically and morphologically heterogeneous. Curr Opin Solid State Mater Sci 2005;9:202-210.

[22] Arpón R, Narciso J, García-Cordovilla C, Louis E, Molina JM, Saravanan RA. Threshold pressure for infiltration and particle specific surface area of particle compacts with bimodal size distributions. Scripta Mater 2004;51:623-627.

[23] Cowan RD. Pulse method of measuring thermal diffusivity at high temperatures. J App Physics 1963;34:926-927.

[24] Hasselman DPH, Bhatt H, Donaldson KY, Thomas Jr J R. Effect of Fiber Orientation and Sample Geometry on the Effective Thermal Conductivity of a Uniaxial Carbon Fiber-Reinforced Glass Matrix Composite. J Comp Mater 1992;26:2278-2288.

[25] Carslaw HS, Jaeger JC. Heat conduction in solids. Clarendon Press, Oxford, 1959.

[26] Bhatt H, Donaldson KY, Hasselman DPH, Chyung K, Taylor M P. Effect of fibre orientation on the thermal conductivity of a uniaxial carbon fibre-reinforced aluminoborosilicate glass-matrix composite for various specimen geometries. J Mater Sci Lett 1991;10:1267-1270.

[27] Molina JM, Prieto R, Narciso J, Louis E. The effect of porosity on the thermal conductivity of Al–12wt.%Si/SiC composites. Scripta Mater 2009;60:582-585.

[28] Swartz ET, Pohl RO. Thermal boundary resistance. Rev Mod Phys 1989;61:605-668.

[29] Liu DM, Lin BW. Thermal conductivity in hot-pressed silicon-carbide. Ceram Int 1996;22:407-414.

[30] Prasher R. Thermal boundary resistance and thermal conductivity of multiwalled carbon nanotubes. Phys Rev B 2008;77:075424.

[31] Garrett KW, Rosenberg HM. The thermal conductivity of epoxy-resin / powder composite materials. J Phys D: Appl Phys 1974;7:1247-1258.

[32] Shackelford JF, Alexander W. Materials Science and Engineering Handbook. 3rd edition, CRC Press, 2001

[33] Kaye & Laby. Tables of physical and chemical constants. National Physical Laboratory; online source: http://www.kayelaby.npl.co.uk/. Accessed last time in March 2015.

FIGURE CAPTIONS

Figure 1. Micrographs of the graphite flakes (a) and SiC particles (b), used as reinforcements in the present work.

Figure 2. Illustration of samples cut at different angles with the flakes plane. z' is the axis along which uniaxial packing pressure was applied (it corresponds to the direction perpendicular to the basal planes of flakes); z is the axis along which the thermal conductivity is measured. Sample dimensions were 60×30×10 mm (top) cut from the

infiltrated preform of dimensions 60×60×30 mm, while small samples for testing had 20 mm in height and a square section of side 10 mm (middle and bottom).

Figure 3. Micrographs of the composites obtained through infiltration of Al-12Si alloy into a preform containing 54% graphite flakes plus 29% SiC particles of average diameter 22.5 μm (referred as D7 preform – see Table 1).

Figure 4. Images showing the measurement processes carried out on micrographs of the composites in order to obtain the volume fraction of phases over screening windows of increasing size (a) and the misalignment of the graphite flakes in respect to the reference cutting angle (b).

Figure 5. (a) Volume fraction of flakes V_f as a function of the size of the square field over which it was evaluated for five series of independent measurements on micrographs of composites obtained through infiltration of Al-12Si alloy into a preform containing 54% graphite flakes plus 29% SiC particles of average diameter 22.5 μm (referred as D7 preform). Results obtained starting either on flakes (filled symbols) or on the metallic composite (empty symbols) are shown. The straight broken line corresponds to the bulk value of V_f ; (b) Standard deviation of many measurements such as those of the upper panel.

Figure 6. Frequency profiles of graphite flakes orientation angles in respect to two samples with cutting angles of θ_m=0º (filled symbols) and θ_m=45º (empty symbols). The lines are fittings with the Gaussian function ($\mathbf{f(x) = ae^{-\frac{(x-b)^2}{2c^2}}}$, with $\mathbf{a = \frac{1}{c\sqrt{2\pi}}}$) with c (standard deviation) parameter equal to 12º for both series of data corresponding to θ_m=0º and θ_m=45º.

Figure 7. A graph of results calculated with the disk-like flakes model versus experimental results for the thermal conductivity (TC) of the ternary G_f-SiC_p/Al–12Si (filled symbols) and G_f-SiC_p/epoxy (empty symbols) composites. (a) corresponds to the TC along graphite flakes while (b) corresponds to the TC measured transversally to (a). The line represents the identity function. The results were obtained for a value of the particle volume fraction in the Al-12Si–SiC_p composite of 0.55, which does actually represent the average of the two limiting bounds for the particle content in the ternary composite, namely 0.52 and 0.58 (see main text).

Figure 8. Experimental thermal conductivity of G_f-SiC_p/Al-12Si (a) and G_f-SiC_p/epoxy (b) composites for samples cut along a direction forming an angle θ (degrees) with the flakes plane. Results for TC measured either by the RSST (empty symbols) or LFT (filled symbols) techniques are shown (see text). (a) and (b) correspond to the TC along and transversally to the graphite planes, respectively.

TABLE LEGENDS

Table 1. Thermal conductivity K_c (W/mK) of samples cut along a direction parallel (K_c^L) and perpendicular (K_c^T) to the flakes plane (see Figure 2) for G_f-SiC_p/Al-12Si and G_f-SiC_p/epoxy composites. The measurements were carried out with the RSST technique.

Table 2. Material parameters used in the calculations according to Equations (1-10). K_r^{in} is the intrinsic thermal conductivity while h is the interfacial thermal conductance.

Table 3. Thermal conductivity K_c (W/m·K) of samples cut along a direction forming an angle θ with the flakes plane (see Figure 2). K_c was measured with the RSST (1) and LFT (2) techniques - see text for details.

FIGURES

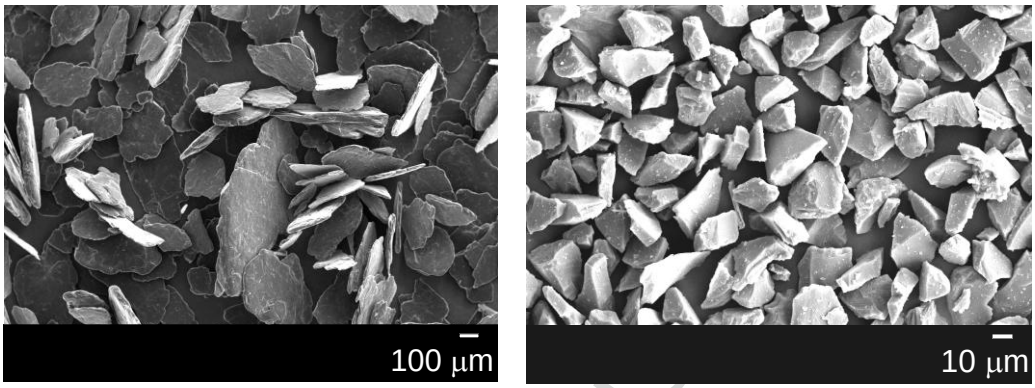

(a) (b)

Figure 1

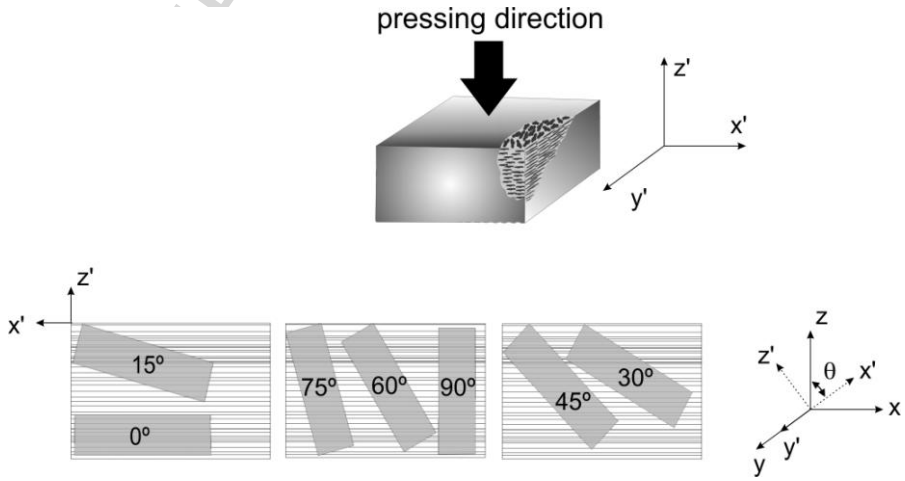

Figure 2

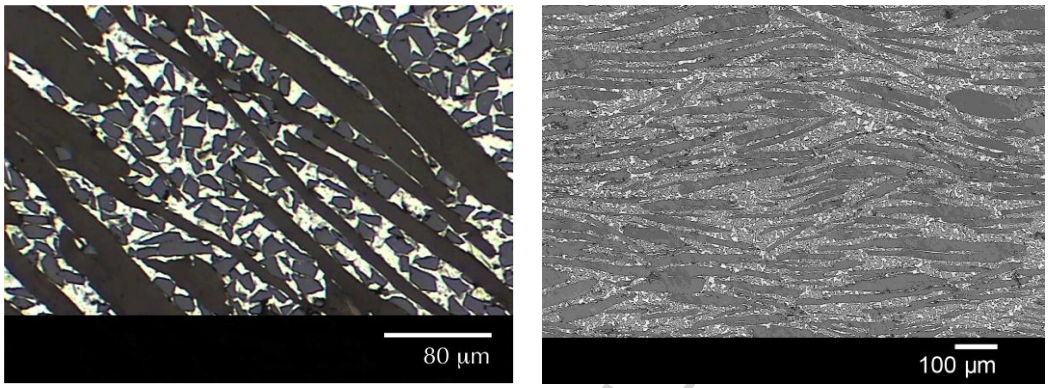

Figure 3

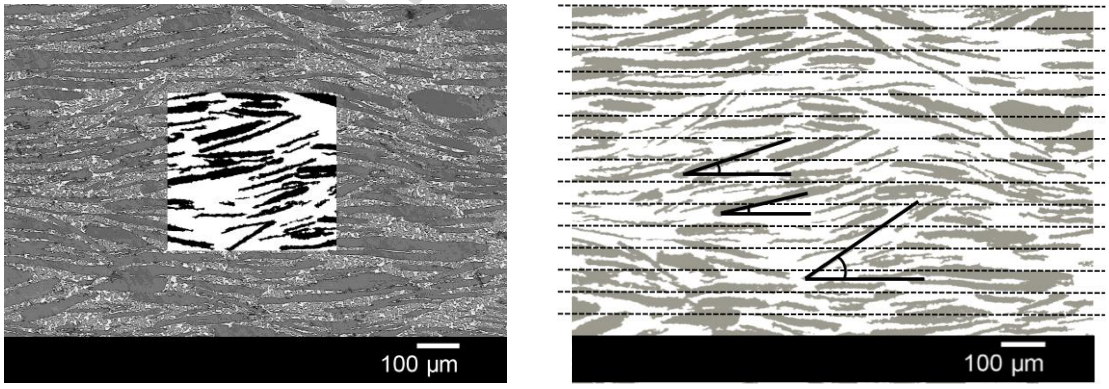

(a) (b)

Figure 4

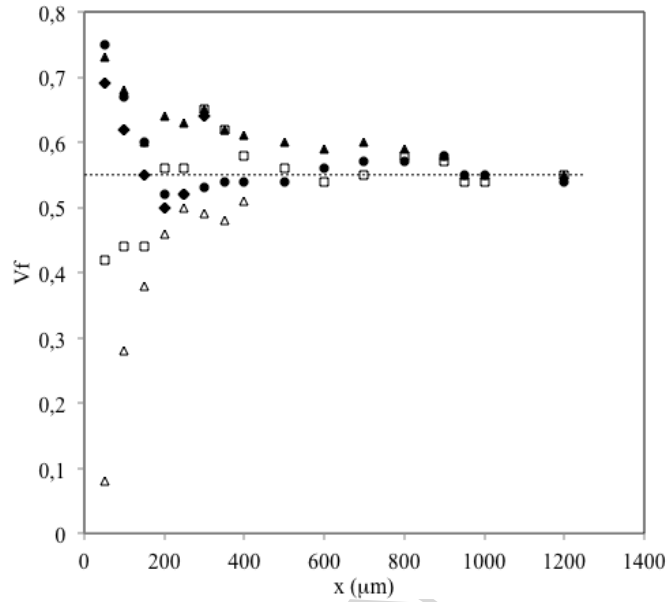

(a)

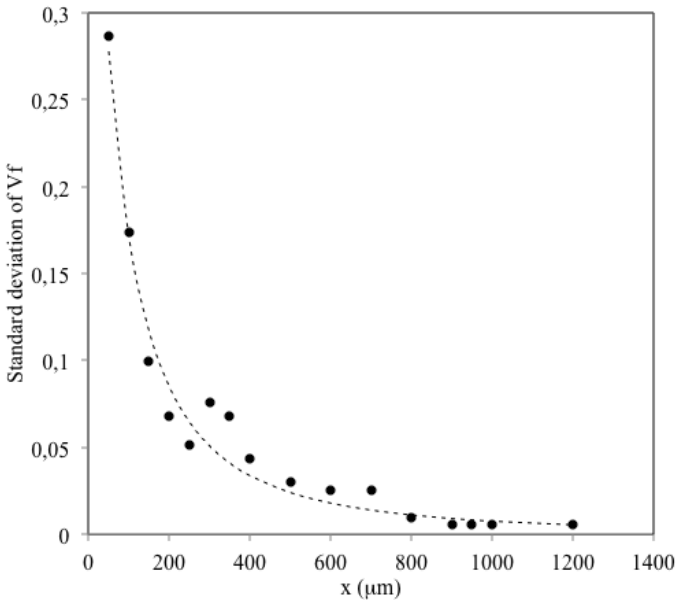

(b)

Figure 5

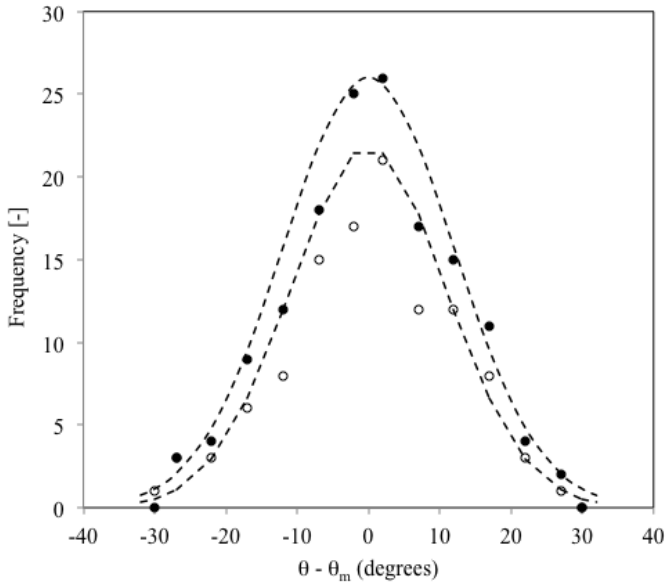

Figure 6

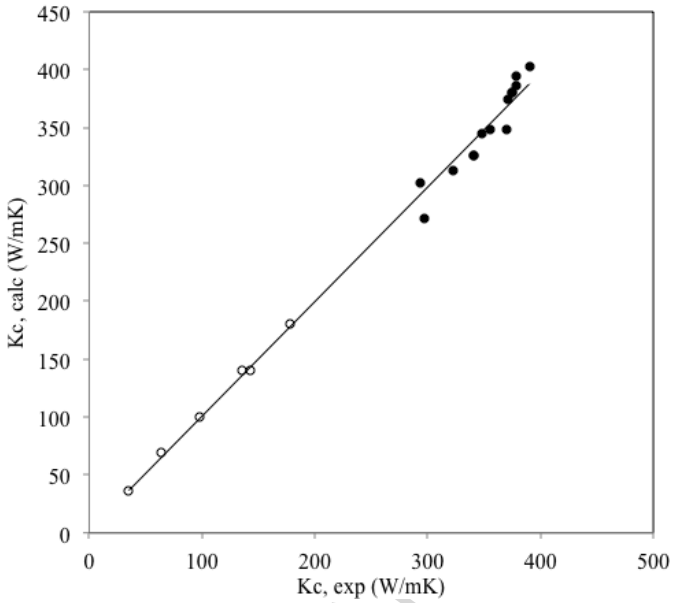

(a)

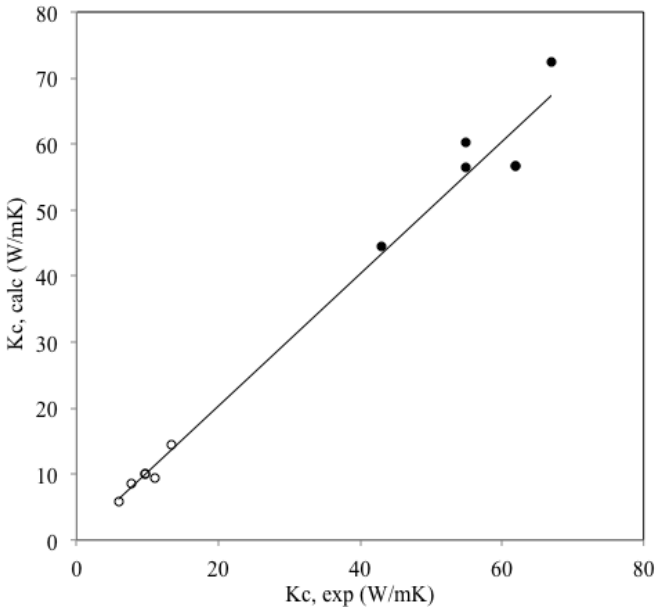

(b)

Figure 7

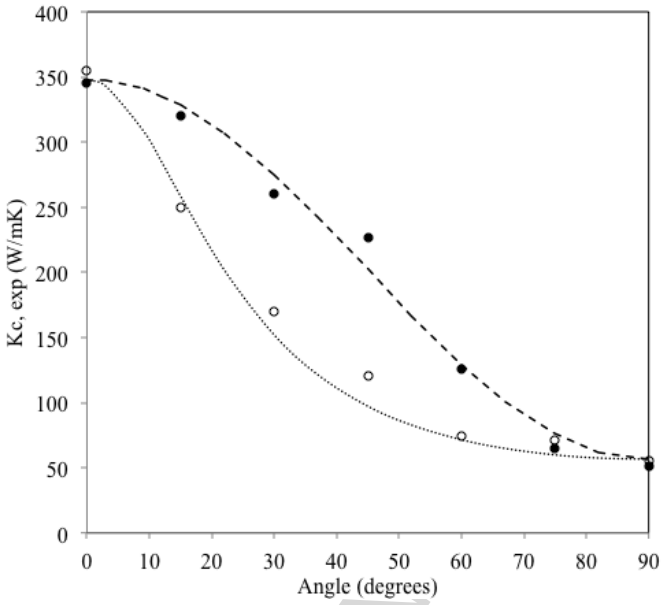

(a)

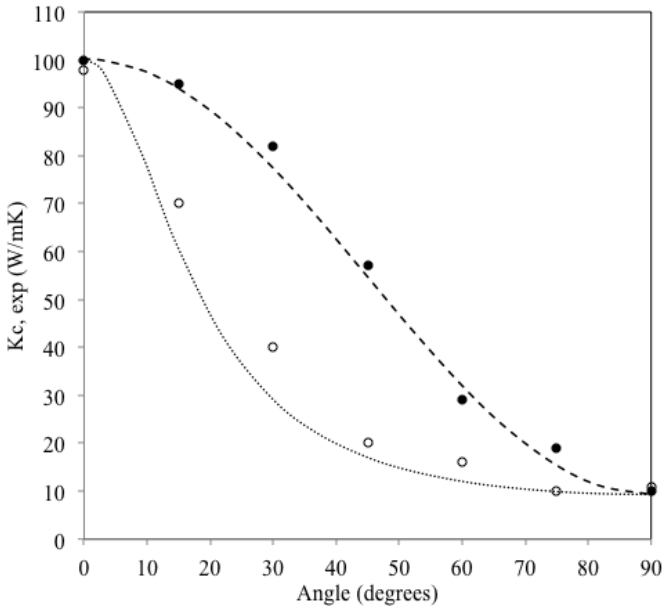

(b)

Figure 8

TABLES

Table 1. Thermal conductivity K_c (W/mK) of samples cut along a direction parallel (K_c^L) and perpendicular (K_c^T) to the flakes plane (see Figure 2) for G_f-SiC_p/Al12Si and G_f-SiC_p/epoxy composites. The measurements were carried out with the RSST technique.

Preform code	D (μm)	V_{SiC}	V'_{SiC}	V_f	Matrix			
					Al-12Si		Epoxy	
					K_c^L	K_c^T	K_c^L	K_c^T
A1	167	0.20	0.58	0.62	378	-	-	-
B1	60.2	0.24	0.56	0.58	371	-	178	13.4
C1	37	0.26	0.55	0.52	370	55	-	-
D1	22.5	0.21	0.55	0.63	375	-	135	9.6
D2	22.5	0.16	0.55	0.69	390	-	-	-
D3	22.5	0.19	0.55	0.63	375	-	143	9.6
D4	22.5	0.23	0.55	0.53	348	-	-	-
D5	22.5	0.29	0.55	0.44	322	-	64	7.8
D6	22.5	0.34	0.55	0.41	294	-	-	-
D7	22.5	0.29	0.55	0.54	355	55	98	11
E1	12.7	0.16	0.52	0.67	378	43	-	-
E2	12.7	0.28	0.52	0.51	341	62	-	-
E3	12.7	0.34	0.52	0.36	297	67	35.2	5.9

.

Table 2. Material parameters used in the calculations according to Equations [1-10]. K_r^{in} is the intrinsic thermal conductivity while h is the interfacial thermal conductance.

	Materials			Matrix-reinforcement couples			
	Al-12Si	Epoxy	SiC	Al-12Si/SiC	Al-12Si/Gf	Epoxy-SiC	Epoxy-Gf
K_r^{in} (W/mK)	179 [27]	1.7 *	254 [23]	-	-	-	-
h (W/m^2K)	-	-	-	6.39×10^{7} ** [28,29]	5.41×10^{7} ** [28,30]	1.69×10^{6} ** [31,29]	1.37×10^{6} ** [31,30]

*value provided by the supplier; **values estimated from the well-known acoustic mismatch model [28], using the Debye velocities for matrix and reinforcement encountered in the coupled of cited references, respectively, and the densities and heat capacities found in [32]; the heat capacity for the epoxy resin in cured condition was taken from [33].

Table 3. Thermal conductivity K_c (W/m·K) of samples cut along a direction forming an angle θ with the flakes plane (see Figure 2). K_c was measured with the RSST (1) and LFT (2) techniques - see text for details.

Preform code	Angle	Matrix			
		Al-12Si		Epoxy	
		K_c (1)	K_c (2)	K_c (1)	K_c (2)
D7	0	355	345	98	100
	15	250	320	70	95
	30	170	260	40	82
	45	120	227	20	57
	60	74	126	16	29
	75	71	65	10	19
	90	55	51	11	10

Highlights of manuscript entitled

Anisotropy in thermal conductivity of graphite flakes-SiC_p/matrix composites: implications in heat sinking design for thermal management applications

signed by J.M. Molina and E. Louis

- Anisotropy in thermal conductivity of graphite flakes-based composites is evaluated.
- Samples are cut in a direction forming a variable angle with the oriented flakes.
- For angles 0º and 90º, thermal conductivity does not depend on sample geometry.
- For intermediate angles, thermal conductivity strongly depends on sample geometry.
- "Thin" samples must be thicker than 600 μm, "thick" samples must be encapsulated.